https://doi.org/10.33307/entomon.v51i1.1618
Entomon 51(1): 89-96
Article No. ent. 51112

Analysis on the chemical spectra of *Acraea terpsicore* Linnaeus, 1758 and *Parantica aglea* (Stoll, [1782]) (Lepidoptera, Nymphalidae) wing scales

Amina Thaj and G. Prasad*

Department of Zoology, University of Kerala, Kariavattom, Thiruvananthapuram, Kerala, 695581, India.
Email: aminathaj2@gmail.com; probios1@gmail.com

ABSTRACT: The wing scale chemical spectra of two nymphalid species, *Parantica aglea* and *Acraea terpsicore* was investigated using Fourier Transform Infrared Spectroscopy (FTIR) to determine characteristic functional groups. Comparative analysis of the functional groups revealed the presence of several major groups, including alcohols, phenols, aldehydes, alkanes, alkenes, alkyl halides, alkynes, methylene, acids, nitro compounds, primary, secondary, and tertiary amines, esters, ethers, polysulfides, aryl disulfides, cyanide and thiocyanate ions, carbonate ions, organic sulphates, organic nitrates, nitrate ions, aromatic ethers, aromatic phosphates, phosphate ions, ammonium ions, silicate ions, transition metal carbonyls, and organic siloxanes or silicones. Common functional groups between the two species include alcohols and phenols, alkanes, alkenes, alkyl halides, methylene, acids, esters, ethers, aryl disulfides, cyanide and thiocyanate ions, carbonate ions, organic nitrates, nitrate ions, phosphate ions, and silicate ions. However, certain elements are specific to particular regions, such as alkynes. This study represents the first FTIR analysis conducted on the wing scales of *P. aglea* and *A. terpsicore* providing valuable insights into their chemical compositions.

KEY WORDS: Functional groups, chemical compositions, FTIR, specific to regions

INTRODUCTION

Butterflies, with their captivating wing coloration, encompass various pigmentary, structural, and androconial scales, crucial for functions such as camouflage and mate attraction (Das *et al*., 2017). The vibrant coloration observed on butterfly wings arises from the combination of microstructures and particular pigments present within them and the pigments exhibit vivid colours as a result of their selective absorption and reflection of light at specific wavelengths, with the residual energy being dissipated as heat (Shamim *et al*., 2014; Sharmila *et al*., 2020).

In our study, a comparative spectroscopic analysis of wing scales of two Nymphalid species of butterflies namely *Acraea terpsicore* Linnaeus, 1758 and *Parantica aglea* (Stoll, [1782]) was conducted using Fourier-Transform Infrared Spectroscopy (FTIR) to elucidate the functional groups. *P. aglea* belongs to subfamily Danainae and has wings with a mesmerizing combination of black and white stripes whereas *A. terpsicore* that belongs to subfamily Heliconiinae is a medium sized butterfly with wings displaying a rich tawny-orange colour with intricate black markings. FTIR spectroscopy enables the identification of molecular structures by analyzing the vibrational frequencies

* Author for correspondence

of functional groups. Optical studies on *P. aglea* and *A. terpsicore* has been conducted by Thaj and Prasad, (2025) using Ultraviolet–Visible Near-Infrared Spectroscopy. Limited studies have been conducted on arthropods such as honeybees and dragonflies using FTIR analysis (Machovic *et al*., 2017), and only a few reports exist on FTIR analysis in butterflies (Tian *et al*., 2015; Krishna *et al*., 2020).

MATERIALS AND METHODS

Specimens of *P. aglea* and *A. terpsicore* were collected from Kariavattom Campus, University of Kerala, Thiruvananthapuram (8°32', 8° 34'N; 76° 52', 76° 54'E). The species was identified following Kunte *et al*. (2026). The study is made partially following the methodology of Archana *et al*. (2022). Functional groups of dorsal black and white regions of *P. aglea* forewing and dorsal orange and spot region of *A. terpsicore* hindwing was selected for the study (Fig. 1). The selected regions were cut using clean scissors and the regions of about 0.5cm sample size was isolated and studied by placing on FTIR spectroscopy (Smart Orbit™ Thermoscientific Nicolet iS50). The method employed is Attenuated total reflection (ATR) method where the sample can be placed directly without any special preparation and the spectrum was obtained between 400-4000cm^{-1}in the mid IR region. The wavenumbers of FTIR peaks obtained is compared using frequency chart and it is graphically represented by origin 2023b software (https://www.originlab.com/).

RESULTS AND DISCUSSION

Analysis of the functional groups in *P. aglea* and *A. terpsicore* of dorsal side revealed comparable spectral features with peaks occurring at similar positions irrespective of the region studied; however, minor variations are observed in the peak intensities (Fig. 2). On analysing the FTIR peaks of *P. aglea* black region, the black coloured region shows peaks at wavenumbers 3725.89, 3269.48, 2918.26, 2849.70, 2161.84, 2018.64, 1625.73, 1540.77, 1456.75, 1374.95, 1307.76, 1238.44, 1156.81, 1065.89, 509.74, 491.18 and 465.52cm^{-1}. The corresponding functional groups are alcohol with weak stretch, H- bonded OH stretch, acid (O-H) stretch, amide (N-H) stretch, methylene (C-H) asymmetric stretch, alkane (C-H) stretch, methylene (C-H) symmetric stretch, methoxy, methyl ether weak stretch, aldehyde (=C-H) stretch, cyanide ion and thiocyanate ions, alkynes, aryl substituted C=C stretch, primary amine and secondary amine (NH bend), organic nitrates, organic chain azo(-N=N-), alkene (C=C) stretch, aromatic ring, aliphatic nitro compounds, aromatic stretch, nitro stretch, carbonate ion, alkanes, organic sulfates, nitro stretch, carboxylic acid salt, alkyl halide (C-F) stretch, amine (C-N) stretch, aromatic ethers, aromatic phosphates, alkyl halide (C-F) stretch, ether (C-O) stretch, acid (C-O) stretch, ester (C-O) stretch, secondary amine (CN stretch), tertiary amine (CN stretch), cyanate ion, aliphatic fluoro compounds, phosphate ion, silicate ion, alcohol (C-O) stretch, aliphatic iodo compounds, alkyl halide (C-Br) stretch, polysulfides and aryl disulfides.

The peaks of *P. aglea* white region are observed at wavenumbers 3726.37, 3266.45, 2917.36, 2849.15, 2076.51, 1624.29, 1540.94, 1462.01, 1371.06, 1157.50, 1072.19, 1027.69, 953.48, 898.72, 763.61, 575.53 and 467.62cm^{-1}. Functional groups observed on white region are alcohol (O-H) stretch, ammonium ion, acid (O-H) stretch, amide (N-H) stretch, methylene C-H asymmetric stretch, alkane (C-H) stretch, methoxy, cyanide ion, thiocyanate ion, alkenyl C=C stretch, secondary amine (NH) bend, open chain imino(-C=N-), open chain azo (-N=N-), organic nitrates, alkene (C=C) stretch, aliphatic nitro compounds, methylene C-H bend, carbonate ion, phenol or tertiary alcohol (OH) bend, organic sulfates, nitrate ion, alkane, alkyl halide (C-F) stretch, secondary amine and tertiary amine (CN stretch), cyanate and sulfonates, ether and ester (C-O) stretch, cyclohexane ring vibrations, skeletal C-C vibrations, aliphatic phosphates, organic siloxane, silicate ion, alkene(C-H) bending, aliphatic chloro compounds, alkyl halide (C-Cl) stretch, aliphatic iodo compounds (C-I), alkyl halides (C-Br) stretch and aryl disulfides.

Analysis on the *A. terpsicore* hindwing orange region specifies peaks at 3726.70, 3271.68, 2918.06,

Table 1. Wavenumbers and their corresponding functional groups of *P. aglea* and *A. terpsicore*

Hydrocarbons and functional groups	Spectral peak values (cm^{-1})			
	P. aglea		*A. terpsicore*	
	Black region	White region	Orange region	Spot region
Alcohols and Phenols	3725.89, 3269.48	3726.37, 3266.45, 1371.06, 1072.19	3726.70, 3271.68	3725.78
Aldehydes	2849.70	Not detected	Not detected	2849.01
Alkanes	2918.26, 1456.75	2917.36, 1462.01, 1371.06	2918.06, 1458.75,	2917.34, 1457.15, 1376.82
Alkenes	1625.73	1624.29, 953.4 8, 898.72, 763.61	1624.94	1625.56
Alkyl halides	1307.76, 1156.81, 1065.89 (C-F), 509.74 (C-Br)	1371.06, 1072.19, 1027.69 (C-F), 763.61(C-Cl), 575.53(C-Br)	1375.94, 1235.13, 1023.73(C-F), 526.41(C-Br)	1376.82, 1235.31, 1023.77(C-F), 526.71(C-Br)
Alkynes	2161.84	Not detected	Not detected	Not detected
Methylene	2918.26, 2849.70, 1456.75	2917.36, 2849.15, 1462.01	2918.06, 2849.37, 1458.75	2917.34,2849.01, 1457.15
Acid	3269.48, 2918.26, 2849.70, 1238.44	3266.45, 2917.36, 2849.15	2849.37, 1235.13	3268.96, 2917.34, 2849.01, 1235.31
Carboxylic acid	1307.76	Not detected	1375.94	1376.82
Nitro compounds	1540.77	1540.94, 1371.06	1375.94, 1540.88	Not detected
Primary, secondary and tertiary amines	1625.73, 1156.81	1624.29, 1157.50, 1072.19	Not detected	1023.77
Ester	1238.44, 1156.81, 1065.89	1157.50, 1072.19, 1027.69	1235.13, 1023.73	1235.31, 1023.77
Ether	1238.44, 1156.81, 1065.89	1157.50, 1072.19, 1027.69	1235.13, 1023.73	1023.77
Polysulfides	491.18	Not detected	465.83	Not detected
Aryl disulfides	465.52	467.62	495.04	464.87
Cyanide and thiocyanate ion	2161.84	2076.51, 1157.50	2049.82	2039.91
Carbonate ion	1456.75	1462.01	1458.75	1457.15
Organic sulfates	1374.95	1371.06	Not detected	Not detected
Organic nitrates	1625.73	1624.29	1624.94,	1625.56
Nitrate ion	1374.95	1371.06	1375.94	1376.82
Aromatic ethers	1238.44	Not detected	Not detected	Not detected
Aromatic phosphates	1238.44	Not detected	1235.13	Not detected
Phosphate ion	1065.89	1072.19, 1027.69,	1023.73	1023.77
Ammonium ion	Not Detected	3266.45	3271.68	3268.96
Silicate ion	1065.89	1072.19, 1027.69, 953.48	1023.73	1023.77
Transition metal carbonyls	Not detected	Not detected	2049.82, 1980.80	1980.99
Organic siloxane or silicone	Not detected	1027.69	1023.73	1023.77

2849.37, 2049.82, 1980.80, 1624.94, 1514.45, 1458.75, 1375.94, 1235.13, 1023.73, 526.41, 495.04, and 465.83cm^{-1} (Table 1). The corresponding functional groups are alcohol (O-H) weak stretch, ammonium ions weak stretch, methylene (C-H) asymmetric stretch, alkane (C-H) stretch, methylene (C-H) symmetric stretch, methoxy, methyl ether O-CH_3, (C-H) stretch, cyanide ion, thiocyanate ion, transition metal carbonyls, alkenyl (C=C) stretch, open chain azo (-N=N-) stretch, open chain imino (-C=N-) stretch, organic nitrates, alkene (C=C) stretch, aromatic (C=C) stretch, methyl (C-H) asymmetric bend, methylene (C-H) bend, carbonate ion, alkane (-C-H) bending, carboxylate, aliphatic nitro compounds, nitrate ion, alkyl halide (C-F) stretch, aromatic phosphates, amine (C-N) stretch, ether (C-O) stretch, acid (C-O) stretch, ester (C-O) stretch, cyclohexane ring vibrations, aliphatic flouro compounds (C-F) stretch, aliphatic phosphates (P-O-C) stretch, organic siloxane, aliphatic iodo compounds (C-I) stretch, aryl disulfides and polysulfides with broad peaks.

On *A. terpsicore* spot region the respective peaks formed are at wavenumbers 3725.78, 3268.96, 2917.34, 2849.01, 2039.91, 1980.99, 1625.56, 1540.88, 1457.15, 1376.82, 1235.31, 1023.77, 526.71 and 464.87cm^{-1} (Table 1). Here the functional groups observed are alcohol (O-H) stretch, H-bonded O-H stretch, ammonium ion, acid (O-H) stretch, amide (N-H) stretch, methylene (C-H) asymmetric stretch, alkane (C-H) stretch, methylene (C-H) symmetric weak and broad stretch, methoxy, methyl ether O-CH3 weak stretch, aldehyde (=C-H) stretch, cyanide ion, thiocyanate ion, transition metal carbonyls weak stretch, open chain azo (-N=N-) stretch, organic nitrates weak and broad stretch, alkene (C=C) stretch, weak and broad peaks showing aliphatic and aromatic nitrocompounds, aromatic (C=C) stretch, carbonate ion, alkane (-C-H) bending, aromatic (C=C) stretch in which the peaks are weak and symmetric, alkyl halide (C-F) stretch, acid (C-O) stretch, ester (C-O) stretch in which the peaks are broad and weak, cyclohexane ring vibrations, primary amine (C-N) stretch, aliphatic phosphates (P-O-C) stretch, organic siloxane, phosphate ion, ether (C-O) stretch, alkyl halides (C-Br) stretch and aryl disulfides (S-S stretch) that shows broad and weak peaks.

A comparative region-wise analysis of functional group distribution in *P. aglea* and *A. terpsicore* (Table 1) reveals the presence of alcohol groups across multiple wing regions in both species. In *P. aglea*, alcohol-related peaks were recorded at 3725.89 and 3269.48 cm^{-1} in the black region, and at 3726.37, 3266.45, 1371.06, and 1072.19 cm^{-1} in the white region. Similarly, *A. terpsicore* exhibited alcohol peaks at 3726.70 and 3271.68cm^{-1} in the orange region and at 3725.78cm^{-1} in the spot region, indicating that alcohol groups are common to all regions examined.

Aldehyde groups were detected at 2849.70 cm^{-1} exclusively in the black region of *P. aglea* and were absent in its white region. Likewise, aldehydes were not observed in the orange region of *A. terpsicore* but were present in the spot region of the hindwing at 2849.01cm^{-1}, suggesting a region-specific distribution.

Alkanes functional groups were identified in both black and white regions of *P. aglea*, with peaks at 2918.26 and 1456.75cm^{-1} in the black region and at 2917.36, 1462.01, and 1371.06cm^{-1} in the white region. Correspondingly, *A. terpsicore* showed alkane peaks at 2918.06 and 1458.75cm^{-1} in the orange region and at 2917.34, 1457.15 and 1376.82 cm^{-1} in the spot region.

Alkene groups were present in both species across the studied regions. In *P. aglea*, alkenes were identified at 1625.73cm^{-1} in the black region and at 1624.29, 953.48, 898.72 and 763.61cm^{-1} in the white region. In *A. terpsicore*, alkene peaks were observed at 1624.94cm^{-1} in the orange region and at 1625.56cm^{-1} in the spot region.

Alkyl halides were detected in all examined regions of both species. In *P. aglea*, characteristic peaks appeared at 1307.76, 1156.81, 1065.89 and 509.74cm^{-1} in the black region and at 1371.06, 1072.19, 1027.69, 763.61 and 575.53cm^{-1} in the white region. In *A. terpsicore*, alkyl halide peaks were observed at 1375.94, 1023.73, and 526.41 cm^{-1} in the orange region and at 1376.82, 1235.31, 1023.77 and 526.71cm^{-1} in the spot region.

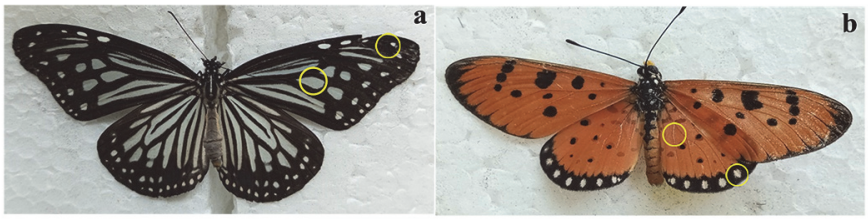

Fig. 1 (a) *Parantica aglea;* (b) *Acraea terpsicore* (Yellow circles represent the region of study)

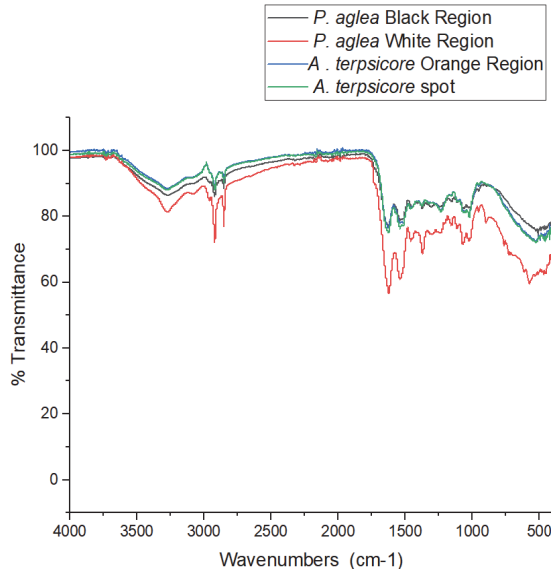

Fig. 2 FTIR spectra of *P. aglea* and *A. terpsicore*

Alkyne functional groups were detected only in the black region of *P. aglea* at 2161.84cm^{-1}. Methylene groups were consistently observed in all regions of both species, with characteristic peaks around 2918.26, 2849.70, and 1456.75, 2917.36, 2849.15, 1462.01, 2918.06, 2849.37, 1458.75, 2917.34, 2849.01 and 1457.15cm^{-1}. Acid functional groups were also identified across regions, showing peaks at 3269.48, 2918.26, 2849.70, 1238.44, 3266.45, 2917.36, 2849.15, 2849.37, 1235.13, 3268.96, 2917.34, 2849.01 and 1235.31cm^{-1}. Carboxylic acid groups were present in all regions except the white region of *P. aglea*, with notable peaks at 1307.76, 1375.94 and 1376.82cm^{-1}.

Nitro compounds were absent only in the spot region of *A. terpsicore*, while all other regions exhibited nitro-related peaks ranging from 1540.77, 1540.94, 1371.06, 1375.94 and 1540.88cm^{-1}. Ester and ether groups were identified in all studied regions, with ester peaks occurring between 1238.44, 1156.81, 1065.89, 1157.50, 1072.19, 1027.69, 1235.13, 1023.73, 1235.31 and 1023.77 cm^{-1}, while ether groups were observed within a spectral range of 1238.44, 1156.81, 1065.89, 1157.50, 1072.19, 1027.69, 1235.13, 1023.73 and 1023.77cm^{-1}. Polysulfides were not detected in the white region of *P. aglea* nor the spot region of *A. terpsicore*, but were present in other regions with peaks at 491.18 and 465.83cm^{-1}. Aryl disulfides were observed consistently across all regions, showing peaks at 465.52, 467.62, 495.04 and 464.87cm^{-1}.

Other region-wise functional groups and their corresponding spectral peaks are summarized (Table 1). From the study, some elements appear common to all the regions studied such as alcohols, alkanes, alkenes, alkyl halides, methylene, acid, ester, ether, aryl disulfides, cyanide and thiocyanate ion, carbonate ion, organic nitrates, nitrate ion, phosphate ion and silicate ion (Table 1). Similar observations were reported in the FTIR analysis of *Leptosia nina* wing scales by Thaj and Prasad (2024). In addition, X-ray dot mapping of *A. terpsicore* indicated that carbon and oxygen are the predominant elements (Thaj and Prasad, 2024).

The functional groups can play many roles in the physiology of insects. Akanes acts as water barrier and has hydrophobic property (Drijfhout *et al*., 2009). The presence of alkynes is an important diagnostic tool because only a few organic compounds show absorption in this region (Archana *et al*., 2022). Carboxylic acid plays an important role as anti-desiccation agent and water proofing

agent (Chung and Carroll, 2015). When analysing the presence of alkyl halide, it is observed as one of the major elements present in all regions studied. As per previous reports alkyl halides are compounds that carbon group banded with halogen and they act as sex pheromones, kairomones and anti-aphrodisiac agent (Gibbs and Pomonis, 1995; Chung and Carroll, 2015).

These components are involved in communication and signalling, nest- mate recognition, task-specific cues, dominance and fertility cues, chemical mimicry, mate selection and kin recognition (Archana *et al*., 2022). Differentiating cryptic species poses a frequent challenge in taxonomy and even species that are morphologically identical can be distinguished by their hydrocarbon profiles (Schlick-Steiner *et al*., 2006). Additionally, butterfly wings have attracted extensive scientific attention due to their striking coloration, hydrophobicity, natural fluorescence, self-cleaning properties, mechanical flexibility, and low weight (Kaspar *et al*., 2019; Krishna *et al*., 2020; Devi *et al*., 2021). Also, Cuticular hydrocarbons contribute to thermoregulation, mate recognition, and predator avoidance (Archana *et al*., 2022).

Chitin is a key structural component of the insect cuticle and plays an essential role in the formation of butterfly wing scales and their colour patterns (Nakazato and Otaki, 2023). Structurally, chitin consists of a linear chain of ß(1-4)-linked N-acetylglucosamine (GlcNAc) units with the repeating formula [CHON]™ (Muthukrishnan *et al*., 2012). In the FTIR spectra, the amides, O–H/ N–H stretching along with C–O–C stretching vibrations shows the presence of chitin backbone.

There were no significant differences detected in the chemical composition of the differently coloured wing regions of the two nymphalid species examined in the present study. Similar observations were previously reported by Archana *et al*. (2022), who suggested that colour variation in butterfly wings does not arise mainly from differences in cuticular hydrocarbons, but is instead largely governed by variations in microstructural features such as scales, ridges, and grooves. This interpretation aligns with the concept that the visual appearance of butterfly wings emerges from the collective arrangement of numerous microscopic scales of specific colours, producing species-specific patterns comparable to pointillist art (Nijhout, 1991).

In nymphalid butterflies, wing scales are typically flattened, sac-like structures consisting of a lower lamina connected to an upper lamina bearing ridges and crossribs through trabeculae (Ghiradella, 1998; 2010). The thin-film optical properties of the lower lamina play a dominant role in defining scale colour, with reflectance spectra closely tuned to the underlying pigmentation and overall wing coloration is further modulated by the stacked arrangement of neighbouring scales (Stavenga *et al*., 2014).

Pigment distribution plays a crucial role in butterfly wing coloration that possess functional groups. Melanin is consistently associated with black scales across butterfly taxa, white scales are often assumed to lack pigments, pierid butterflies possess leucopterin in these scales, which primarily absorbs ultraviolet radiation. The yellow, orange, and red scales of pierids, on the other hand, contain xanthopterin and/or erythropterin pigments that selectively absorb violet and blue wavelengths (Kayser, 1985; Wijnen *et al*., 2007).

Scale coloration arises from the combined influence of wavelength-selective pigment absorption and structural light reflection, resulting in reflectance spectra that are largely complementary to pigment absorbance profiles, the absorbance characteristics of ommochrome pigments in nymphalid wings have been experimentally demonstrated through methanol extraction studies in *Precis coenia* (Nijhout, 1997).

In addition, butterflies are widely recognised as sensitive ecological indicators (Ghazanfar *et al.*, 2016), due to their highly delicate and responsive wings (Han *et al*., 2014), even subtle chemical changes in the scales can reflect environmental stress and ecosystem health.

Recent ecological investigations have shown that minor chemical variations in insect cuticles can serve as indicators of environmental pressures such as pollution and climate variability. Studies on *Danaus*

plexippus have revealed complex patterns of metal incorporation in wings, demonstrating the potential of elemental and chemical analyses for assessing environmental contamination, metal toxicity, micronutrient dynamics, and insect movement patterns (Reich *et al*., 2023). Furthermore, phenotypic changes in butterfly wing coloration have been linked to adaptive ecological and evolutionary responses to climate change (MacLean *et al*., 2016). In this context, comparative FTIR analysis of butterfly wing scales emerges as a powerful and sensitive tool for monitoring ecological disturbances and evaluating ecosystem health.

Beyond ecological relevance, insights into natural chemical functional groups have inspired numerous biomimetic innovations. For instance, the specialised surface chemistry underlying the adhesive properties of gecko feet has led to the development of switchable dry–wet self-peeling adhesives (Zhang *et al*., 2021). Understanding the chemical foundations of such biological architectures is therefore essential for translating natural designs into functional engineering materials. Consequently, the present study not only contributes to the limited knowledge of butterfly wing-scale chemistry but also provides a valuable framework for integrating spectrochemical analysis with ecological monitoring and biomimetic material development.

ACKNOWLEDGEMENTS

Authors acknowledge Department of Science & Technology, Government of India for financial support vide reference no: DST/ WISE-PhD/LS/ 2024/271(G) under 'WISE Fellowship for Ph.D.' programme to carry out this work and Central Laboratory of Instrumentation and Facilitation (CLIF), University of Kerala for the instrument facility.

REFERENCES

Archana B., Sharmila E. Joy, Snegapriya M., Rangesh K. and Susaritha S. (2022) Fourier transform infra-red spectrochemical analyses of Pieridae butterfly wings. ENTOMON 47(1): 103–112. doi:10.33307/ entomon.v47i2.709.

Chung H. and Carroll S.B. (2015) Wax, Sex and the origin of species: Dual role of Insect's hydrocarbons in adaptation and mating. Bioassays 37(7): 822–830. doi: 10.1002/bies.201500014.

Das Se., Nachimuthu Shanmugam, Ajay Kumar and Seiko Jose (2017) Potential of biomimicry in the field of textile technology. Bioinspired, Biomimetic and Nanobiomaterials 6(4): 1–42. doi:10.1680/ jbibn.16.00048.

Devi A., Sharmila E.J., Rangesh K., Susaritha S. and Archana B. (2021) Population dynamics of *Catopsilia pyranthe* in Butterfly Garden. Indian Journal of Ecology 48(3): 748–750.

Drijfhout F.P., Kather R. and Martin S.J. (2009) The role of cuticular hydrocarbons in insects. In: Behavioral and Chemical Ecology (Eds. Wen Zhang and Hong Liu), Nova Science Publishers, New York. pp123–145.

Ghazanfar M., Malik M.F., Hussain M., Iqbal R and Younas M. (2016) Butterflies and their contribution in ecosystem: A review. Journal of Entomology and Zoology Studies 4(2) 115–118.

Ghiradella H. (1998) Hairs, bristles, and scales. In Microscopic Anatomy of Invertebrates, 11 A: Insecta (ed. Locke M.), New York, Wiley-Liss. pp257–287.

Ghiradella H. (2010) Insect cuticular surface modifications: scales and other structural formations. Advances In Insect Physiology 38: 135–180. doi: 10.1016/S0065-2806(10)38006-4.

Gibbs A. and Pomonis J.G. (1995) Physical properties of insect cuticular hydrocarbons: The effect of chain length, methyl-branching and unsaturation. Comparative Biochemistry and Physiology, Part B, Biochemistry and Molecular Biology 112(2): 243–249. doi: 10.1016/0305-0491(95)00081-X.

Han Z., Niu, S., Yang M., Mu Z., Bo Li., Zhang J., Ye J. and Ren L. (2014). Unparalleled sensitivity of photonic structures in butterfly wings. RSC Advances 4(85): 45214–45219. doi: 10.1039/ C4RA06117A.

Kaspar P., Sobola D., Sedlák P., Holcman V. and Grmela L. (2019) Analysis of color shift on butterfly wings by Fourier transform of images from atomic force microscopy. Microscopy Research and Technique 82 (12): 2007–2013. doi: 10.1002/ jemt.23370

Kayser H. (1985) Pigments. In: Comprehensive Insect Physiology, Biochemistry and Pharmacology, Vol. 10 (ed. Kerkut G. A., Gilbert L. I.), Oxford, Pergamon

Press. pp367–415.

Krishna X., Nie A.D., Warren J.E., Llorente-Bousquets A.D., Briscoe and Lee J. (2020) Infrared optical and thermal properties of microstructures in butterfly wings. Proceedings of the National Academy of Sciences USA 117(3): 1566–1572.

Kunte K., Sondhi S. and P. Roy (2026) Butterflies of India. v. 4.31. Indian Foundation for Butterflies Trust. URL: https://www.ifoundbutterflies.org.

Machoviè V., Lapèák L., Havelcová M., Borecká L., Novotná M., Novotná M., Javùrková I., Langrová I., Hájková Š., Bro•ová A. and Titìra D. (2017) Analysis of European honeybee (Apis Mellifera) wings using ATR-FTIR and raman spectroscopy: A pilot study. Scientia Agriculturae Bohemica 48(1): 22–29. doi: 10.1515/sab-2017-0004

MacLean H.J., Kingsolver J.G. and Buckley L.B. (2016) Historical changes in thermoregulatory traits of alpine butterflies reveal complex ecological and evolutionary responses to recent climate change. Climate Change Responses 3(1): 91–114. doi: 10.1186/s40665-016-0028-x.

Muthukrishnan S., Merzendorfer H., Arakane Y. and Kramer K. (2012) Chitin metabolism in insects, In: Insect Molecular Biology and Biochemistry. pp193–235.

Nakazato Y. and Otaki J.M. (2023) Live detection of intracellular chitin in butterfly wing epithelial cells in vivo using fluorescent brightener 28: implications for the development of scales and color patterns. Insects 14(9): 753. doi:10.3390/insects14090753.

Nijhout H.F. (1991) The Development and Evolution of Butterfly Wing Patterns. Washington, DC, Smithsonian Institution Press.

Nijhout H.F. (1997) Ommochrome pigmentation of the *linea* and *rosa* seasonal forms of *Precis coenia* (Lepidoptera: Nymphalidae). Archives of Insect Biochemistry and Physiology 36: 215–222.

Reich M.S., Kindra M., Dargent F., Hu L., Flockhart D.T.T., Norris D.R., Kharouba H., Talavera G., Bataille C.P. (2023) Metal and metal isotopes incorporation in insect wings: Implications for geolocation and pollution exposure. Frontiers in Ecology and Evolution11. doi: 10.3389/fevo.2023.1085903.

Schlick-Steiner B.C., Steiner F.M., Moder K., Seifert B., Sanetra M., Dyreson E., Stauffer C. and Christian E. (2006) A multidisciplinary approach reveals cryptic diversity in Western Palearctic Tetramorium ants (Hymenoptera: Formicidae). Molecular Phylogenetics and Evolution 40(1): 259–273. doi: 10.1016/j.ympev.2006.03.005

Shamim G., Ranjan S.K., Pandey D.M. and Ramani R. (2014) Biochemistry and biosynthesis of insect pigments. European Journal of Entomology 111(2): 149–164. doi: 10.14411/eje.2014.021.

Sharmila J.E., Thatheyus A.J., Susaritha S. and Snehapriya M. (2020) Seasonality of butterflies in Alagar Hills reserve forest, India. ENTOMON 45(1): 53–60. doi: 10.33307/entomon.v45i1.503

Stavenga D.J., Leertouwer H.L. and Wilts B.D. (2014) Coloration principles of nymphaline butterflies – thin films, melanin, ommochromes and wing scale stacking. Journal of Experimental Biology 217 (12): 2171–2180. doi: 10.1242/jeb.098673.

Thaj A. and Prasad G. (2024) Chemical features of forewing scales of *Leptosia nina* Fabricius, 1793 (Lepidoptera: Pieridae). Applied Biological Research 26(1): 130–135. doi: 10.48165/abr.2024.26.01.11

Thaj A. and Prasad G. (2024) X-ray dot map of major surface elements in three common Indian butterflies. Journal of Entomological Research 48(2): 282–285. doi: 10.5958/0974-4576.2024.00056.8.

Thaj A., Prasad G. (2025) EXPRESS: Analysis of the Optical Properties of Butterflies Using Ultraviolet–Visible Near-Infrared Spectroscopy. Applied Spectroscopy 80(2): 198–207. doi: 10.1177/00037028251397426.

Tian X., Song G., Ding X., Jiajun G.U., Liu Q., Zhang W., Su H., Kang D., Qin Z. and Zhang D. (2015) Photonic structure arrays generated using butterfly wing scales as biological units. Journal of Materials Chemistry B 3(9):1743–1747. doi: 10.1039/c4tb01691b.

Wijnen B., Leertouwer H. L. and Stavenga D. G. (2007) Colors and pterin pigmentation of pierid butterfly wings. Journal of Insect Physiology 53(12): 1206–1217. doi: 10.1016/j.jinsphys.2007.06.016.

Zhang Y., Ma S., Li Bin., Yu Bo., Lee H., Cai M., and Gorb S.N., Zhou F. and Liu W. (2021) Gecko's feet-inspired self-peeling switchable dry/wet adhesive. Chemistry of Materials 33(8): 2785–2795

(Received November 27, 2025; revised ms accepted February 10, 2026; published March 31, 2026)